BILINGUAL PUBLISHING GROUP

Journal of Environmental & Earth Sciences
https://journals.bilpubgroup.com/index.php/jees

ARTICLE

Comparison of Machine Learning Methods for Satellite Image Classification: A Case Study of Casablanca Using Landsat Imagery and Google Earth Engine

***Hafsa Ouchra*[1*], *Abdessamad Belangour*[1], *Allae Erraissi*[2]**

[1] *Laboratory of Information Technology and Modeling LTIM, Hassan II University, Faculty of Sciences Ben M'sik, Casablanca, 20670, Morocco*

[2] *Chouaib Doukkali University, Polydisciplinary Faculty of Sidi Bennour, El Jadida, 24000, Morocco*

ABSTRACT

Satellite image classification is crucial in various applications such as urban planning, environmental monitoring, and land use analysis. In this study, the authors present a comparative analysis of different supervised and unsupervised learning methods for satellite image classification, focusing on a case study in Casablanca using Landsat 8 imagery. This research aims to identify the most effective machine-learning approach for accurately classifying land cover in an urban environment. The methodology used consists of the pre-processing of Landsat imagery data from Casablanca city, the authors extract relevant features and partition them into training and test sets, and then use random forest (RF), SVM (support vector machine), classification, and regression tree (CART), gradient tree boost (GTB), decision tree (DT), and minimum distance (MD) algorithms. Through a series of experiments, the authors evaluate the performance of each machine learning method in terms of accuracy, and Kappa coefficient. This work shows that random forest is the best-performing algorithm, with an accuracy of 95.42% and 0.94 Kappa coefficient. The authors discuss the factors of their performance, including data characteristics, accurate selection, and model influencing.

Keywords: Supervised learning; Unsupervised learning; Satellite image classification; Machine learning; Google Earth Engine

*CORRESPONDING AUTHOR:
Hafsa Ouchra, Laboratory of Information Technology and Modeling LTIM, Hassan II University, Faculty of Sciences Ben M'sik, Casablanca, 20670, Morocco; Email: ouchra.hafsa@gmail.com

ARTICLE INFO
Received: 27 August 2023 | Revised: 27 October 2023 | Accepted: 31 October 2023 | Published Online: 14 November 2023
DOI: https://doi.org/10.30564/jees.v5i2.5928

CITATION
Ouchra, H., Belangour, A., Erraissi, A., 2023. Comparison of Machine Learning Methods for Satellite Image Classification: A Case Study of Casablanca Using Landsat Imagery and Google Earth Engine. Journal of Environmental & Earth Sciences. 5(2): 118-134. DOI: https://doi.org/10.30564/jees.v5i2.5928

1. Introduction

Accurate classification of satellite images plays an essential role in many fields such as urban management, environmental planning, precision agriculture, and natural resource monitoring [1]. With the rapid advance of machine learning, a wide range of methods has emerged to automate this complex and crucial task [2].

Casablanca, a dynamic and constantly growing metropolis, faces complex challenges in urban management and sustainable development. Accurate classification of satellite imagery [3] in this region is a major challenge to enable informed decisions on planning, land use, and environmental preservation. For these challenges, machine learning methods offer promising prospects by providing tools for extracting meaningful information from large amounts of imagery data.

In this context, this study proposes to compare machine learning methods for satellite image classification [4,5], focusing on a case study carried out in Casablanca using Landsat imagery data. This study aims to evaluate and compare the performance of different machine learning methods in the context of satellite image classification, using Landsat 8 OLI data [6] from Casablanca. We examine supervised learning methods [7] such as support vector machines (SVMs) [8] and random forest (RF) [9], gradient tree boost (GTB) [10], etc., as well as unsupervised learning methods [2] such as K-means [11] and Lvq [12] using the Google Earth Engine platform [13]. By evaluating these methods through appropriate performance metrics, we aim to identify the most suitable method for accurate land use classification in a complex urban environment.

The importance of this study lies in its contribution to the scientific literature, offering essential information to practitioners and researchers engaged in satellite image classification. The results of this study could guide the choice of appropriate methods for specific applications in urban areas like Casablanca. In addition, this research could inspire future improvements in the design of hybrid methods or the exploration of deep learning techniques to meet the increasingly complex challenges of satellite image classification.

In the following sections, we detail the machine learning methods examined, the data used in this study, experimental protocols, and evaluation metrics. Finally, we present and discuss in depth the results obtained, while highlighting the implications and future perspectives arising from this in-depth comparison of machine learning methods for satellite image classification in Casablanca.

2. Related work

Numerous studies in the scientific literature have focused on land cover classification using various machine learning techniques [14], including CART [15], SVM [8], and random forest [9] classifiers for supervised learning. **Table 1** provides an overview of other related works.

Yang et al. [16] highlighted the advantages of automated monitoring programs based on remote sensing, such as early change detection, informed decision-making, and wide spatial coverage, making them valuable tools for resource management and decision-making.

Wahbi et al. [17] highlighted the evolution from simple algebraic methods to artificial intelligence-based techniques [18,19], such as machine learning and deep learning [20], to generate accurate and useful settlement data. They highlighted the challenge of information extraction and image classification, proposing a system for assigning classes to pixels in the input image.

Phan et al. [21] demonstrated that satellite image time series gave higher classification accuracies than single-date images in land cover studies over the last decade. They noted the importance of Google Earth Engine (GEE) in remote sensing applications due to its efficient temporal aggregation methods and cloud-based nature.

Although the literature review [14,22-24] indicates extensive research on land cover classification using GEE and various algorithms in European and Asian regions, there is little specific research for Morocco. This review is an opportunity for researchers to ex-

plore land cover classification in Casablanca, Morocco, using supervised and unsupervised algorithms by exploiting the advantages of the GEE platform [13,25].

For unsupervised learning methods, previous work [11,26-28] highlights the ability of unsupervised learning to autonomously identify and categorize distinct land-use classes, offering a data-driven approach to land-use analysis.

Land cover mapping in urban environments has received particular attention due to the challenges associated with dynamic and heterogeneous urban settings [29]. Previous studies have highlighted the complexity of urban land cover analysis, including spectral heterogeneity, mixed pixels, and temporal changes [30]. They also demonstrated the usefulness of Landsat data for urban land use analysis, leading to a better understanding of urban growth and dynamics [31].

This research makes a valuable contribution to the field by examining six supervised and two unsupervised machine learning algorithms to broaden our understanding of land use dynamics in the region and to promote more comprehensive land use studies specific to the city of Casablanca and to compare in terms of accuracy and Kappa coefficient the effectiveness of each algorithm for the classification of different areas of Casablanca.

Table 1. Overview of related work.

Classification methods	Datasets satellite	Better methods from researcher study	References
● Maximum Likelihood ● Minimum Distance ● Mahalanobis Distance	Landsat 7 ETM+ data	Maximum likelihood	[32]
● ISODATA ● Maximum Likelihood ● Hybrid Method	Desert Outlay Datasets	Hybrid method	[33]
● Minimum Distance ● Maximum Likelihood ● K-Nearest Neighbour	IRIS Plants Dataset	K-Nearest neighbour	[34]
● Maximum Likelihood ● Minimum Distance ● Parellelpiped ● Maximum Likelihood	Landsat 7 ETM+ Images	Maximum likelihood	[35]
● Support Vector Machine ● Maximum Likelihood ● Mahalanobis Distance ● Minimum Distance ● Spectral Information Divergence ● Binary Codes ● Parallelepiped	Landsat 7 ETM+ data	Support vector machine	[36]
● Random Forest ● Classification and regression tree ● Gradient tree boost ● Support vector machine ● Minimum distance ● Decision tree	Landsat 8 OLI	Minimum distance	[14]

3. Study area and datasets

3.1 Casablanca study area

The study area for this research encompasses the vibrant urban landscape of Casablanca, a prominent coastal city in Morocco. As the largest city in the country, Casablanca represents a dynamic hub of economic, cultural, and social activities. It is geographical features, urban expansion, and diverse land uses make it an ideal case study for evaluating and comparing machine learning methods for satellite

image classification.

Casablanca's geographical coordinates range from 33.5441° N latitude to 7.5864° W longitude. The city is situated along the northwestern coast of Morocco, overlooking the Atlantic Ocean as shown in **Figure 1**. The study area includes the densely populated urban core, and the surrounding suburban regions, capturing the intricacies of different land cover types and their interactions.

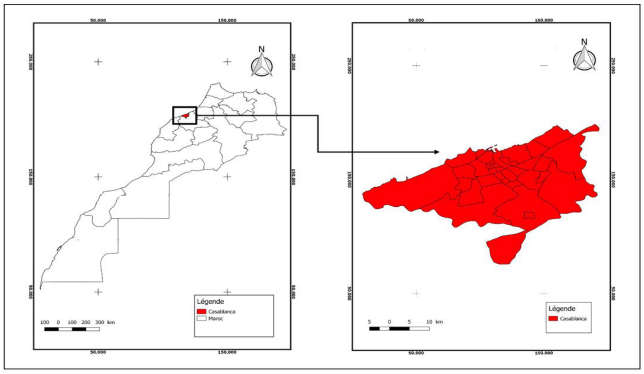

Figure 1. Casablanca study area.

3.2 Landsat 8 OLI dataset

Landsat imagery serves as the primary data source for this study. The Landsat satellites provide multispectral images with different wavelength bands, enabling the extraction of valuable information about land cover, vegetation, water bodies, and urban structures. These images have been collected over specific time frames, allowing the assessment of seasonal variations and changes in land use. This study collects Landsat images from 1-1-2021 to 31-12-2021.

The complex urban environment of Casablanca presents a rich array of land cover classes, including residential areas, industrial zones, commercial districts, green spaces, water bodies, and transportation networks. The diversity of these classes poses a significant challenge for accurate satellite image classification, highlighting the importance of selecting appropriate machine learning methods and techniques.

This study utilized Landsat 8 OLI satellite imagery for land cover mapping in the designated study area. For land cover classification, the study obtained reflectance data from Landsat 8 OLI image bands spanning from January 1, 2021, to December 31, 2021. These images had a spatial resolution of 30 meters for bands B1 to B7. They were captured every 16 days using the GEE cloud platform, which offered data availability, storage, and advantages.

4. Methodology

Through the utilization of the methodology illustrated in **Figures 2 and 3**, researchers can proficiently employ both supervised and unsupervised machine learning algorithms for the classification of Landsat satellite images within the Google Earth Engine platform, enabling them to gain valuable insights into the dynamics of land use change and make informed decisions about urban planning and environmental management [37]. Invariably, the first step of data pre-processing is shared between the methodologies of supervised and non-supervised algorithms.

● Data acquisition and preprocessing

We obtained Landsat 8 OLI satellite imagery [38] for the target region, Casablanca, Morocco, from the Google Earth Engine data catalogue [13], then pre-processed and filtered the imagery to correct for atmospheric distortions and radiometric calibration, to ensure data quality and consistency. We then selected January 1, 2021, to December 31, 2021, to capture the different land cover conditions and changes over time.

4.1 Workflow of supervised methods

● Data preparation and feature extraction

After the data acquisition stage, we moved on to the data preparation and feature extraction stage, in which we defined five land cover classes (built-up area, cropped area, forest area, barren area, and water body) based on the study objectives and the specific characteristics of our study area, these classes are presented in **Table 2**. Next, we created a representative training dataset by selecting sample pixels from the pre-processed imagery for each land-use class. The samples had to be accurately labeled using ground truth data or existing land cover maps.

Then we extracted from the Landsat 8 OLI imagery the spectral bands and indices that distinguish the different land cover types. The most common visible bands are B2, B3, and B4, the NIR band is B5 and the short-wave infrared bands are B6 and B7 (**Table 3**).

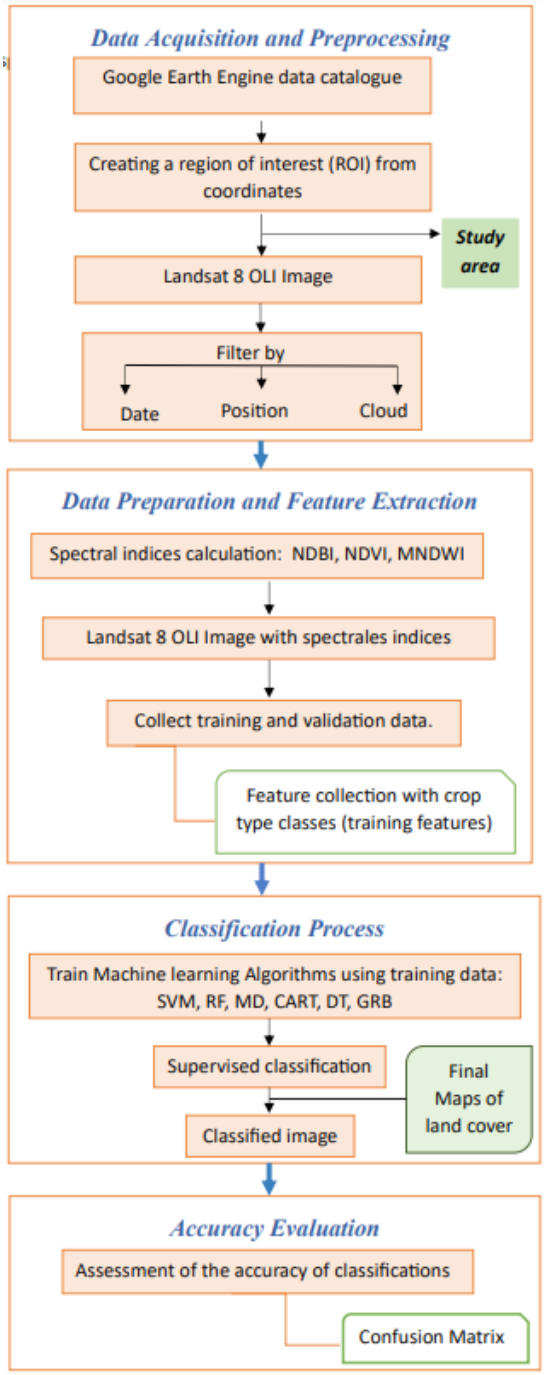

Figure 2. Workflow of the presented method.

● Training the models

In this step, we selected six supervised algorithms to apply a land cover classification of the six classes (built-up area, cropped area, forest area, barren area, and water body) extracted in the previous step. The supervised machine learning algorithms chosen to classify the Casablanca study area are random forest (RF) [9], CART [15], support vector machine (SVM) [8], decision tree (DT) [15], minimum distance (MD) [39], and gradient tree boost (GTB) [10]. **Table 4** provides an overview of the parameters for each algorithm.

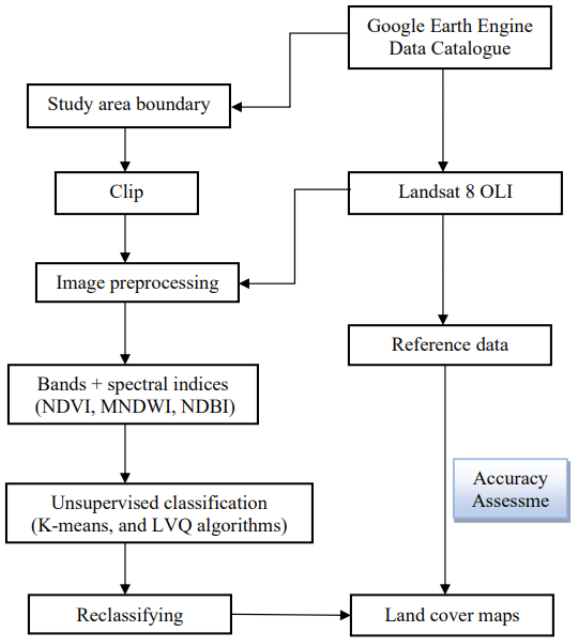

Figure 3. Workflow of methodology implemented in Google Earth Engine (GEE).

These algorithms are implemented in the Google Earth Engine platform using available built-in functions or custom scripts. We trained the supervised algorithms using the prepared training dataset. During training, the algorithms learn to associate the extracted features with the corresponding in these step land-use classes. Note that we have already divided the training data into training (80%) and validation (20%) sets to evaluate model performance during training and avoid over-fitting.

● Model evaluation

We evaluated the performance of the trained models using a validation dataset to measure their accuracy and generalization capabilities. Evaluation measures such as accuracy, producer accuracy, user accuracy, and coefficient Kappa. **Table 5** shows

these metrics.

● Land cover classification

Finally, we generated land-use maps and visualization outputs to evaluate the results and identify classification errors or ambiguities.

A confusion matrix [40] analysis was conducted for each method to evaluate the accuracy of the classified land cover maps generated by the supervised machine learning algorithms in GEE. The confusion matrix provided an overview of the accuracy assessment, and the metrics were presented in **Table A1**.

4.2 Workflow of unsupervised methods

The unsupervised learning methodology for mapping the land cover of Casablanca using Google Earth Engine involves a sequence of steps encompassing data preparation, unsupervised clustering, interpretation, accuracy assessment, and visualization. The integration of Google Earth Engine's capabilities and satellite imagery facilitates efficient and accurate land cover classification within the urban context of Casablanca. The following steps describe the methodology shown in **Figure 3**:

● Region of interest (ROI) selection

Next, we defined the specific area of Casablanca that will be the focus of the classification. The ROI should encompass the land cover types of interest and account for the urban complexity of the city.

● Unsupervised learning algorithm

Subsequently, unsupervised learning algorithms,

Table 2. Land cover classes/references.

Land cover classes	Numbers of points	Description
Water_area	115	A water area refers to a geographical region or surface covered by various types of water bodies, such as oceans, seas, rivers, lakes, ponds, reservoirs, and wetlands.
Forest_area	174	A forest area refers to a large expanse of land characterized by dense vegetation dominated by trees, shrubs, and other woody plants. Forests are vital ecosystems that provide numerous ecological, economic, and social benefits.
Barren_area	150	Barren areas are characterized by minimal or no vegetation cover, and they can be found in various environments
Built-up_area	130	This class represents densely built urban areas with structures, buildings, roads, and other urban infrastructure.
Cropped_area	119	A cropped area, also known as cropland or agricultural land, refers to a specific portion of land that is actively used for cultivating crops and agricultural activities. In such areas, farmers engage in planting, growing, and harvesting various crops to produce food, fiber, and other agricultural products.
Total	688	

Table 3. Bands of Landsat 8 OLI satellite.

Bands			
Name	**Spatial resolution (Pixel size) meters**	**Spectral resolution (μm)**	**Wavelength**
B3	30	0.53-0.59	Green
B4	30	0.64-0.67	Red
B5	30	0.85-0.88	Near infrared (NIR)
B6	30	1.57-1.65	Shortwave infrared (SWIR 1)
B7	30	2.11-2.29	Shortwave infrared (SWIR 2)

Source: [38].

specifically k-means clustering [43], and LVQ [12] are applied to the pre-processed Landsat imagery.

K-means clustering [11] is chosen for its capability to autonomously group pixels with similar spectral characteristics into distinct clusters, representing different land cover classes. The algorithm is initialized with a user-defined number of clusters and iteratively assigns pixels to the nearest cluster centroid based on spectral similarity. Google Earth Engine's cloud-based processing capabilities play a pivotal role in the scalability of the methodology.

LVQ, or learning vector quantization [12], is a supervised learning algorithm, but it always works with unlabeled data; it can also be said to be an unsupervised learning algorithm. It has been used to compare the differences between unsupervised and supervised learning algorithms. It uses a training data set to classify new data points according to their similarity to labeled examples in the training set. In this paper, we used LVQ as an unsupervised cluster-

Table 4. Parameters for each algorithm.

Machine learning algorithms type	Algorithms	Parameters	Description
Supervised algorithms	MD	metric = Mhalanobis	The distance metric to use.
	RF	numberOfTrees = 15	The number of decision trees to create.
	Cart	maxNodes = 15	The maximum number of leaf nodes in each tree
	SVM	kernel = linear	The kernel type. One of LINEAR **(u′×v), POLY ($(\gamma \times u' \times v + coef_0)^{degree}$)**
	DT	treeString	The decision tree, specified in the text format
	GTB	numberOfTrees = 15	The number of decision trees to create.
Unsupervised algorithms	K-means	nCluster = 5	The number of clusters.
		distanceFunction = Euclidean	Distance function to use.
	LVQ	numCluster = 5	The number of clusters.

Table 5. Evaluation metric equations for each classification.

Metrics	Equation	Description
(OA) Overall accuracy	$OA = \frac{\text{Number of correctly classified samples}}{\text{Number of samples}}$	It was used to determine the proportion of correctly mapped reference sites among all reference sites, expressed as a percentage. It was calculated by dividing the number of correctly classified samples by the total number of samples [40,41].
(UA) User accuracy	$UA = \frac{\text{Correct imprevious surface pixel}}{\text{Correct} + \text{Misclassified pixel}}$	It represented the frequency with which the actual terrain features were correctly displayed on the classified map or the probability of correctly classifying a certain land cover in a ground area. It was calculated by dividing the number of accurately classified reference sites for a particular class by the total number of reference sites for that class [34].
(PA) Producer accuracy	$PA = \frac{\text{Correct imprevious surface pixel}}{\text{Total imprevious pixels}}$	It indicated the reliability of the class on the map with respect to its presence in the field. It was calculated by dividing the total number of correct classifications for a specific class by the sum of correct and misclassified pixels for that class [34].
Kappa coefficient	$K = \frac{p_{accord} - P_{Hasard}}{1 - P_{Hasard}}$.	It provided an overall evaluation of the classification performance compared to random assignment. It ranged from –1 to 1 and was derived from a statistical test to evaluate the classification accuracy, determining if the classification performed better than random [42]. ● The observation of inter-rater agreement is: p_{accord} ● The overall probability that graders agree is: P_{Hasard}

ing algorithm to group pixels or data points based on their similarity. The LVQ algorithm in GEE works by iteratively adjusting a set of cluster prototypes to minimize the distance between prototypes and data points. It assigns each data point to the nearest prototype, effectively clustering the data into distinct groups. The platform efficiently computes clustering algorithms across Landsat imagery spatial and temporal coverage of Landsat imagery, enabling rapid analysis of the entire study area.

● Accuracy assessment and validation

Validation and accuracy assessment are integral components of the methodology. A stratified random sampling approach generates reference data points across the study area. These reference points are used to validate the accuracy of the unsupervised classification results. **Table 2** shows the reference data used. Various accuracy metrics, including overall accuracy and kappa coefficient, are calculated to quantify the agreement between the classified land cover map and the reference data.

● Visualization and mapping

The final step of the methodology involves visual interpretation and refinement. The unsupervised classification results are visually compared with high-resolution imagery and existing land cover maps to identify and rectify misclassifications or inconsistencies.

In summary, throughout the methodology, Google Earth Engine's computational capabilities are leveraged for efficient processing, enabling the analysis of large-scale Landsat datasets. The cloud-based nature of the platform facilitates scalability and accelerates data processing to achieve accurate land cover mapping in the urban environment of Casablanca.

5. Results and discussion

5.1 Supervised learning

The study area comprised multiple land cover classes (5 classes), as shown in **Table 2**, which required considerable computational effort in local computation mode.

Various classification methods [8-10,15,39] were applied to map the study area in Casablanca, including random forest (RF), classification and regression trees (CART), gradient tree boosting, support vector machine (SVM), minimum distance (MD), and decision trees (DT). The resulting land cover maps for each approach are displayed in **Figure 4**, and you'll find the legend showing the names of each classified class with its very visible color in **Figure 5**.

The performance of each classification method was evaluated using several metrics [13]: overall accuracy, user accuracy for each class, producer accuracy for each class, and the Kappa coefficient derived from the confusion matrix. The equations utilized for the computation of these metrics are illustrated in **Table A1**.

We have integrated spectral indices with the extracted features and Landsat image bands to guarantee high accuracy for each algorithm. These spectral indices are combinations of pixel values from multiple spectral bands in a multispectral image. These indices provide valuable information about the relative presence or absence of specific land cover types. One widely recognized index is the Normalized Difference Vegetation Index (NDVI) [33]. Besides NDVI, several other indices like the Modified Normalized Difference Water Index (MNDWI), among others, utilize various spectral bands to emphasize different phenomena such as vegetation, water, soil, etc. In this study, we employed three specific spectral indices [33]: NDVI for vegetation, soil, MNDWI for water, and Normalized Difference Built-up Index (NDBI) for built-up areas. **Table 6** outlines the formulas for calculating each of these indices.

This research incorporated the four spectral indices into the feature extraction phase and incorporated them integrated the training data creation process. During this step, the indices were computed and appended as additional spectral bands to enhance the classification outcomes for each classifier utilized in this project. By incorporating these indices, the study aimed to improve the classification accuracy and achieve more precise identification of land cover categories.

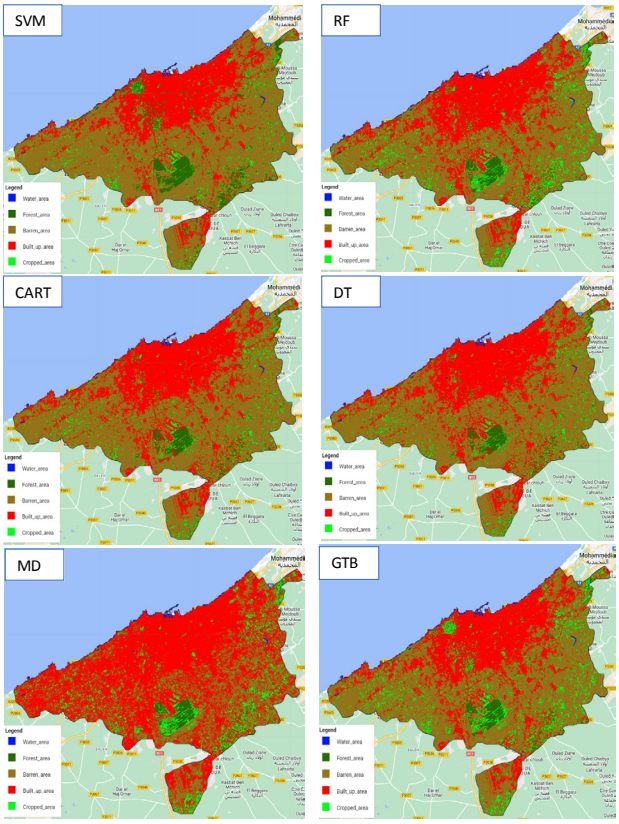

Figure 4. Classification results of Casablanca's land cover map.

Figure 5. Legend of classification results in the land cover mapping of Casablanca.

This study used Landsat 8 OLI datasets and processing tools, including the Google Earth Engine (GEE) platform, to map land cover categories in Casablanca. The study used various classifiers, such as CART, RF, SVM, Gradient Tree Boost, DT, and MD, to delineate the territory into different zones, including Water, Forest, Built-up, Barren, and Cropped areas.

Based on previous studies [9,14,16,19-23,46-52] and our own research, we found that the methodology employed in our experiment can be adapted to map and evaluate different regions in various countries or cities, as this methodology is not oriented solely toward Casablanca city. The main contribution of this research has been the successful adaptation of the method to map and evaluate land use in other regions or countries. Based on the confusion matrix for each classifier, it was evident that the random forest classifier was the most effective, boasting a Kappa coefficient of 0.94. This value is close to 1, indicating that the classification is significantly superior to random. Moreover, it achieved an accuracy of 95.42%, significantly higher than the accuracy of the other classifiers, which were 94.77%, 91.50%, 91.50%, 83%, and 93.46% for MD, DT, CART, SVM, and GTB, respectively. **Figure 6** shows the overall accuracy of these classifiers. The results for the DT and CART classifiers were very similar. However, the SVM classifier exhibited a considerably lower accuracy of 83% compared to the other classifiers, and its Kappa coefficient was 0.78.

Table 6. Spectral indices used.

Index	Equation	References
Normalized difference vegetation index (NDVI)	$\mathrm{NDVI} = \frac{\mathrm{NIR} - \mathrm{RED}}{\mathrm{NIR} + \mathrm{RED}}$	[27]
Modified normalized difference water index (MNDWI)	$\mathrm{MNDWI} = \frac{\mathrm{Green} - \mathrm{SWIR1}}{\mathrm{Green} + \mathrm{SWIR1}}$	[44]
Normalized difference built-up index (NDBI)	$\mathrm{NDBI} = \frac{\mathrm{SWIR} - \mathrm{NIR}}{\mathrm{SWIR} + \mathrm{NIR}}$	[45]

The user and producer accuracy of random forest for a given class was generally different. For example, the built-up class showed a difference between the producer accuracy (84.61%) and user accuracy (91.66%), indicating that some areas were correctly identified as built-up areas. **Table A1** shows the land cover confusion matrix of each classifier. In the confusion matrix of the SVM classifier, which has high accuracy compared to other classifiers, we found the producer's accuracy for the cropped class was 50%. By comparison, **Table A1** reveals that the user

achieved an accuracy of 86.66%. This signifies that only half of the reference cropped areas were accurately identified as such, while 86.66% of the areas classified as cropped were indeed cropped.

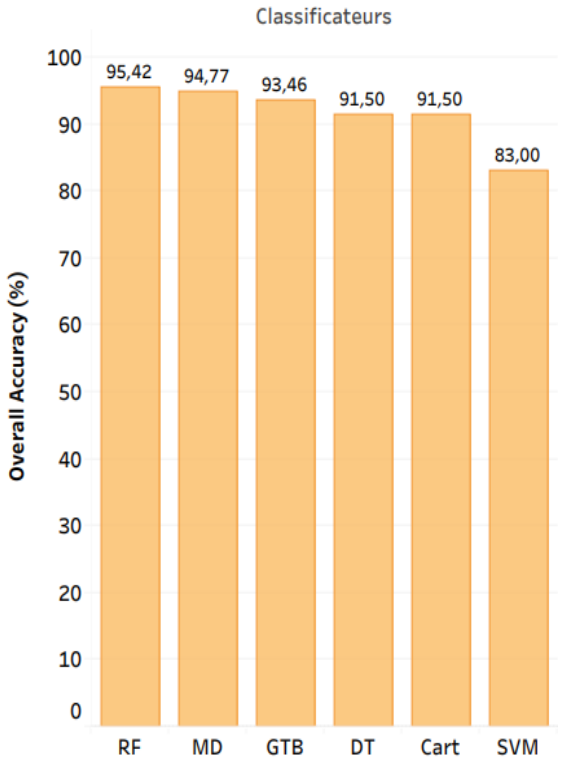

Figure 6. The overall accuracy (OA) of different methods.

The study also incorporated spectral indices, such as NDVI, MNDWI, and NDBI, to enhance land cover classification. These indices were useful in separating different land cover characteristics in Casablanca, including vegetation, water, soil, and built-up areas. Each index had its calculation equation, as detailed in **Table 6**.

Overall, the research demonstrated that some classes achieved high accuracy. In contrast, others had relatively poorer accuracy, indicating the complexity and challenges of land cover classification in diverse regions and environmental conditions.

5.2 Unsupervised learning

This section presents the results and subsequent analysis of the Weka K-means and Lvq algorithm applied in Google Earth Engine (GEE) for land cover mapping of Casablanca using Landsat 8 OLI satellite data for the specified period 1-1-2021 to 31-12-2021. The image was segmented into five distinct land-use classes: water, forest, cultivated areas, barren land, and built-up areas. Performance metrics, including accuracy and Kappa coefficient, provide insight into the effectiveness of these algorithms. **Table 5** shows the equations for these evaluation metrics.

In the Google Earth Engine platform, clusters are used the same way as classifiers. The training data are feature collection properties, fed into the cluster. Unlike classifiers, there is no input class value for a cluster file. The general clustering workflow we followed in this paper is presented in **Figure 3**: First, we collected features with numerical properties in which we searched for clusters, second, we instantiated our cluster and trained the cluster using the training data, then we applied the cluster to the Landsat satellite image of our study area (Casablanca) and finally we labeled the clusters.

In this study, several underlying factors contribute to the accuracy achieved by the K-means and Lvq algorithm:

- Spectral discrimination: The ability of the algorithm to discriminate between land-use classes is highly dependent on the selection of spectral bands and derived indices. Making an informed choice of features with high discriminating power.
- Number of clusters (K): Determining the optimum number of clusters (K) is essentially crucial. An inappropriate choice can lead to classes being merged or split, affecting classification accuracy.
- Spectral similarity: Spectral similarity between certain land use classes can confuse and reduce classification accuracy.

Based on the results obtained by the algorithms used, it can be concluded that unsupervised methods do not achieve optimum performance in the classification and clustering of satellite images for land cover mapping. Supervised approaches, on the other hand, achieve significantly higher accuracy rates. Nevertheless, in the context of this study, considerable efforts have been made to improve the performance of the K-means and Lvq algorithms. Before the application of techniques to improve data quality,

the results of K-means and Lvq had demonstrated particularly low accuracy, amounting to 31.47% and 19.96%, respectively, with a Kappa coefficient of 0.14 and 0.0009, respectively, as shown in **Table 7**. The land-use maps obtained for each algorithm are shown in **Figure 7**.

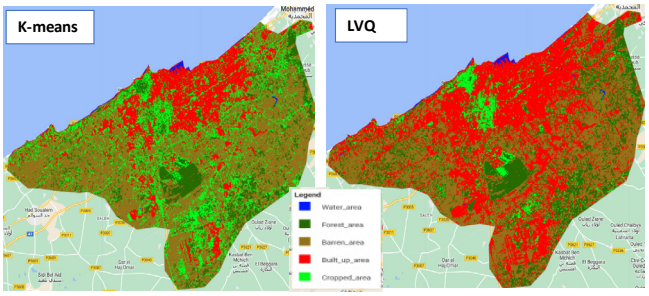

Figure 7. Land cover classification of Casablanca of each algorithm.

To improve these results, a series of improvements were made to the pre-processing stages. Atmospheric correction and cloud removal were applied to enhance source data quality. Next, integrating spectral indices such as NDBI, NDVI, and WNDBI was carried out in conjunction with the image bands. We were incorporating these indices aimed to increase separability between the different classes. **Table 6** shows the equations for these spectral indices.

This approach proved to generate a clear improvement in the accuracy of the K-means algorithm, reaching an accuracy of 38.66% with 0.06 Kappa coefficients, and for the LVQ algorithm, unfortunately, we have a poor accuracy of 26.01% with Kappa coefficients of 0.06. **Figure 8** illustrates these results.

This improvement reflects moderate accuracy but represents significant advances in the initial results. From these results, we can say that the K-means algorithm performs better than the Lvq algorithm, but we concluded that unsupervised learning algorithms do not perform well for land cover mapping. On the other hand, in these previous studies and my previous work [14], we demonstrated that supervised learning algorithms perform well for satellite image classification and land cover mapping.

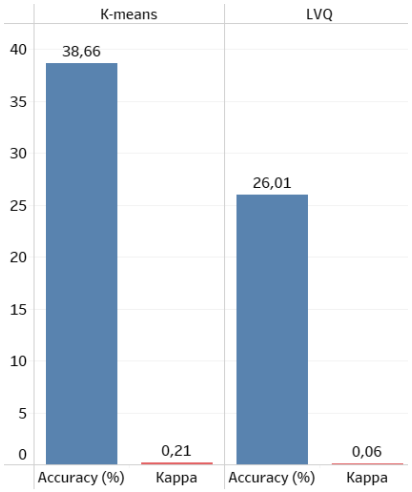

Figure 8. The overall accuracy and Kappa coefficient values of each adopted algorithm.

5.3 Comparison results of supervised and unsupervised methods

According to the results presented in the previous sections, the random forest classifier outperformed the other supervised and unsupervised learning algorithms, achieving an accuracy of 95.42% and a Kappa coefficient of 0.94, indicating its significant superiority over the other classifiers.

The analysis involved comparing the accuracy of each classifier using confusion matrices and various measures such as overall accuracy (OA), user accuracy (UA), producer accuracy (PA), and Kappa coefficient, as shown in **Table 5**. The results showed that the random forest classifier consistently outperformed and outperformed the other algorithms in terms of accuracy and Kappa coefficient, achieving an accuracy of 95.42%, significantly higher than that of the other supervised and unsupervised algorithms, which were 94.77%, 91.50%, 91.50%, 83%, 93.46%, 38.66%, and 26.01% for MD, DT, CART, SVM, GTB, K-means, and Lvq respectively.

As shown in **Table 7**, the SVM classifier showed a significantly lower accuracy of 83% compared to the other supervised algorithms. Its Kappa coefficient was 0.78, while for the non-supervised algorithms, the results indicate that K-means and Lvq showed

particularly low accuracy, amounting to 31.47% and 19.96%, respectively, with Kappa coefficients of 0.14 and 0.0009, respectively.

These results allow us to assert that supervised learning algorithms perform better for land cover mapping than non-supervised learning algorithms. In this work, we have demonstrated that the supervised random forest algorithm outperforms all other algorithms, and that supervised learning algorithms perform well for satellite image classification and land cover mapping.

Table 7. Overall accuracy and Kappa coefficient of each supervised and unsupervised method.

Evaluation metrics	Supervised methods						Unsupervised methods	
	SVM	Cart	RF	GTB	DT	MD	K-means	LVQ
Overall accuracy %	83	91.50	95.42	93.46	91.50	94.77	38.66	26.01
Kappa coefficient	0.78	0.89	0.94	0.91	0.89	0.93	0.21	0.06

6. Conclusions and prospects

In summary, this study highlights the importance of methodological selection in achieving accurate classification of satellite imagery and underlines the need for context-sensitive assessments. The results of this research have significant implications for improving land use mapping, urban planning, and environmental management in similar areas of Casablanca. This study provides useful information for selecting appropriate machine-learning methods for satellite image classification in urban areas like Casablanca. By highlighting the advantages and disadvantages of each technique, we offer practical advice to practitioners and researchers.

This work carried out an in-depth evaluation of various supervised and unsupervised algorithms for the classification of Landsat satellite images in the Casablanca region of Morocco. The aim was to assess the ability of these algorithms to represent various land cover categories. Based on the results presented in this work, accurately the reliability and versatility of the GEE platform, with its cloud-based architecture, eliminates the need to integrate other external and often commercial software. According to the experimental results, the supervised random forest algorithm achieved high accuracy. This success can be attributed to the supervised learning methodology, which involves the collection of training and validation points in the study area. This approach improves the classification process of the study area. This study differs from the existing literature in that previous work has mainly focused on specific phenomena in various study areas in Morocco or other cities and countries.

For future work, the study will explore integrating hybrid methods and exploration of more advanced neural networks, which offer increased efficiency in the classification of satellite images to achieve a more accurate classification of land cover and detection of urban areas in the Casablanca study area in Morocco.

Author Contributions

Hafsa Ouchra designed and processed the data, analyzed the proposed methods, and edited the manuscript; Abdessamad Belangour interpreted and discussed the results; Allae Erraissi revised the manuscript.

Conflict of Interest

All authors have read and agreed to the published version of the manuscript.

Funding

This research received no external funding.

References

[1] Ouchra, H., Belangour, A., Erraissi, A. (editors),

2023. An overview of GeoSpatial Artificial Intelligence technologies for city planning and development. 2023 Fifth International Conference on Electrical, Computer and Communication Technologies (ICECCT); 2023 Feb 22-24; Erode, India. New York: IEEE. p. 1-7.
DOI: https://doi.org/10.1109/ICECCT56650.2023.10179796

[2] Ouchra, H., Belangour, A. (editors), 2021. Satellite image classification methods and techniques: A survey. 2021 IEEE International Conference on Imaging Systems and Techniques (IST); 2021 Aug 24-26; Kaohsiung, Taiwan. New York: IEEE. p. 1-6.
DOI: https://doi.org/10.1109/IST50367.2021.9651454

[3] Ouchra, H., Belangour, A., Erraissi, A., 2022. A comparative study on pixel-based classification and object-oriented classification of satellite image. International Journal of Engineering Trends and Technology. 70(8), 206-215.
DOI: https://doi.org/10.14445/22315381/IJETT-V70I8P221

[4] Ouchra, H., Belangour, A., Erraissi, A. (editors), 2022. Satellite data analysis and geographic information system for urban planning: A systematic review. 2022 International Conference on Data Analytics for Business and Industry (ICDABI); 2022 Oct 25-26; Sakhir, Bahrain. New York: IEEE. p. 558-564.
DOI: https://doi.org/10.1109/ICDABI56818.2022.10041487

[5] Ouchra, H., Belangour, A., Erraissi, A. (editors), 2022. Spatial data mining technology for GIS: A review. 2022 International Conference on Data Analytics for Business and Industry (ICDABI); 2022 Oct 25-26; Sakhir, Bahrain. New York: IEEE. p. 655-659.
DOI: https://doi.org/10.1109/ICDABI56818.2022.10041574

[6] Landsat Data Access [Internet]. U.S. Geological Survey [cited 2022 Aug 20]. Available from: https://www.usgs.gov/landsat-missions/landsat-data-access?qt-science_support_page_related_con=0#qt-science_support_page_related_con

[7] Ouchra, H., Belangour, A., Erraissi, A. (editors), 2022. Machine learning for satellite image classification: A comprehensive review. 2022 International Conference on Data Analytics for Business and Industry (ICDABI); 2022 Oct 25-26; Sakhir, Bahrain. New York: IEEE. p. 1-5.
DOI: https://doi.org/10.1109/ICDABI56818.2022.10041606

[8] Awad, M. (editor), 2021. Google Earth Engine (GEE) cloud computing based crop classification using radar, optical images and Support Vector Machine Algorithm (SVM). 2021 IEEE 3rd International Multidisciplinary Conference on Engineering Technology (IMCET); 2021 Dec 8-10; Beirut, Lebanon. New York: IEEE. p. 71-76.
DOI: https://doi.org/10.1109/IMCET53404.2021.9665519

[9] Magidi, J., Nhamo, L., Mpandeli, S., et al., 2021. Application of the random forest classifier to map irrigated areas using google earth engine. Remote Sensing. 13(5), 876.
DOI: https://doi.org/10.3390/RS13050876

[10] Natekin, A., Knoll, A., 2013. Gradient boosting machines, a tutorial. Frontiers in Neurorobotics. 7, 21.
DOI: https://doi.org/10.3389/fnbot.2013.00021

[11] Ali, I., Rehman, A.U., Khan, D.M., et al., 2022. Model selection using K-means clustering algorithm for the symmetrical segmentation of remote sensing datasets. Symmetry. 14(6), 1149.
DOI: https://doi.org/10.3390/sym14061149

[12] Artelt, A., Hammer, B., 2019. Efficient computation of counterfactual explanations of LVQ models. arXiv preprint arXiv:1908.00735.

[13] Gorelick, N., Hancher, M., Dixon, M., et al., 2017. Google Earth Engine: Planetary-scale geospatial analysis for everyone. Remote Sensing of Environment. 202, 18-27.
DOI: https://doi.org/10.1016/j.rse.2017.06.031

[14] Ouchra, H.A.F.S.A., Belangour, A., Erraissi, A.L.L.A.E., 2023. Machine learning algorithms for satellite image classification using Google Earth Engine and Landsat satellite data: Moroc-

co case study. IEEE Access. 11, 71127-71142.
DOI: https://doi.org/10.1109/ACCESS.2023.3293828

[15] Hu, Y., Dong, Y., 2018. An automatic approach for land-change detection and land updates based on integrated NDVI timing analysis and the CVAPS method with GEE support. ISPRS Journal of Photogrammetry and Remote Sensing. 146, 347-359.
DOI: https://doi.org/10.1016/J.ISPRSJPRS.2018.10.008

[16] Yang, L., Driscol, J., Sarigai, S., et al., 2022. Google Earth Engine and artificial intelligence (AI): A comprehensive review. Remote Sensing. 14(14), 3253.
DOI: https://doi.org/10.3390/RS14143253

[17] Wahbi, M., El Bakali, I., Ez-zahouani, B., et al., 2023. A deep learning classification approach using high spatial satellite images for detection of built-up areas in rural zones: Case study of Souss-Massa region-Morocco. Remote Sensing Applications: Society and Environment. 29, 100898.
DOI: https://doi.org/10.1016/J.RSASE.2022.100898

[18] Taji, K., Ait Abdelouahid, R., Ezzahoui, I., et al. (editors), 2021. Review on architectures of aquaponic systems based on the Internet of Things and artificial intelligence: Comparative study. Proceedings of the 4th International Conference on Networking, Information Systems & Security; 2021 Apr 1-2; KENITRA AA Morocco. New York: Association for Computing Machinery. p. 1-9.
DOI: https://doi.org/10.1145/3454127.3457625

[19] Ouchra, H., Belangour, A., 2021. Object detection approaches in images: A survey. Thirteenth International Conference on Digital Image Processing (ICDIP 2021). 11878, 132-141.
DOI: https://doi.org/10.1117/12.2601452

[20] Ouchra, H., Belangour, A., 2021. Object detection approaches in images: A weighted scoring model based comparative study. International Journal of Advanced Computer Science and Applications(IJACSA). 12(8).

[21] Phan, T.N., Kuch, V., Lehnert, L.W., 2020. Land cover classification using Google Earth Engine and random forest classifier—The role of image composition. Remote Sensing. 12(15), 2411.
DOI: https://doi.org/10.3390/RS12152411

[22] Mahyoub, S., Rhinane, H., Fadil, A., et al. (editors), 2020. Using of open access remote sensing data in google earth engine platform for mapping built-up area in Marrakech City, Morocco. 2020 IEEE International Conference of Moroccan Geomatics, MORGEO; 2020 May 11-13; Casablanca, Morocco. New York: IEEE.
DOI: https://doi.org/10.1109/MORGEO49228.2020.9121912

[23] Sellami, E.M., Rhinane, H.A.S.S.A.N., 2023. A new approach for mapping land use/land cover using Google Earth Engine: A comparison of composition images. The International Archives of the Photogrammetry, Remote Sensing and Spatial Information Sciences. 48, 343-349.
DOI: https://doi.org/10.5194/isprs-archives-XLVIII-4-W6-2022-343-2023

[24] Chemchaoui, A., Brhadda, N., Alaoui, H.I., et al. 2023. Accuracy assessment and uncertainty of the 2020 10-meter resolution land use land cover maps at local scale. Case: talassemtane national park, Morocco.
DOI: https://doi.org/10.21203/rs.3.rs-2953599/v2

[25] Pérez-Cutillas, P., Pérez-Navarro, A., Conesa-García, C., et al., 2023. What is going on within google earth engine? A systematic review and meta-analysis. Remote Sensing Applications: Society and Environment. 29, 100907.
DOI: https://doi.org/10.1016/j.rsase.2022.100907

[26] Jamali, A., 2019. Evaluation and comparison of eight machine learning models in land use/land cover mapping using Landsat 8 OLI: A case study of the northern region of Iran. SN Applied Sciences. 1(11), 1448.
DOI: https://doi.org/10.1007/s42452-019-1527-8

[27] Duda, T., Canty, M., 2002. Unsupervised classification of satellite imagery: Choosing a good algorithm. International Journal of Remote Sensing. 23(11), 2193-2212.

DOI: https://doi.org/10.1080/01431160110078467

[28] Celik, T., 2009. Unsupervised change detection in satellite images using principal component analysis and k-means clustering. IEEE Geoscience and Remote Sensing Letters. 6(4), 772-776.
DOI: https://doi.org/10.1109/LGRS.2009.2025059

[29] Zurqani, H.A., Post, C.J., Mikhailova, E.A., et al., 2019. Mapping urbanization trends in a forested landscape using Google Earth Engine. Remote Sensing in Earth Systems Sciences. 2, 173-182.
DOI: https://doi.org/10.1007/s41976-019-00020-y

[30] Masek, J.G., Huang, C., Wolfe, R., et al., 2008. North American forest disturbance mapped from a decadal Landsat record. Remote Sensing of Environment. 112(6), 2914-2926.
DOI: https://doi.org/10.1016/j.rse.2008.02.010

[31] Duro, D.C., Franklin, S.E., Dubé, M.G., 2012. A comparison of pixel-based and object-based image analysis with selected machine learning algorithms for the classification of agricultural landscapes using SPOT-5 HRG imagery. Remote Sensing of Environment. 118, 259-272.
DOI: https://doi.org/10.1016/j.rse.2011.11.020

[32] Madhura, M., Venkatachalam, S., 2015. Comparison of supervised classification methods on remote sensed satellite data: An application in Chennai, South India. International Journal of Science and Research. 4(2), 1407-1411.

[33] Rozenstein, O., Karnieli, A., 2011. Comparison of methods for land-use classification incorporating remote sensing and GIS inputs. Applied Geography. 31(2), 533-544.
DOI: https://doi.org/10.1016/J.APGEOG.2010.11.006

[34] Kalra, K., Goswami, A.K., Gupta, R., 2013. A comparative study of supervised image classification algorithms for satellite images. International Journal of Electrical, Electronics and Data Communication. 1(10), 10-16.

[35] Akgün, A., Eronat, A.H., Türk, N., 2004. Comparing different satellite image classification methods: an application in Ayvalik District, Western Turkey [Internet]. Available from: https://www.isprs.org/PROCEEDINGS/XXXV/congress/comm4/papers/505.pdf

[36] Niknejad, M., Zadeh, V.M., Heydari, M., 2014. Comparing different classifications of satellite imagery in forest mapping (case study: Zagros forests in Iran). International Research Journal of Applied and Basic Sciences. 8(9), 1407-1415.

[37] Ouchra, H., Belangour, A., Erraissi, A., 2022. A comprehensive study of using remote sensing and geographical information systems for urban planning Internetworking Indonesia Journal. 14(1), 15-20.

[38] Landsat 8 Bands [Internet]. Landsat Science [cited 2023 Oct 26]. Available from: https://landsat.gsfc.nasa.gov/satellites/landsat-8/landsat-8-bands/#

[39] Borra, S., Thanki, R., Dey, N., 2019. Satellite image analysis: Clustering and classification. Springer: Singapore.

[40] Jayaswal, V., 2020. Performance Metrics: Confusion Matrix, Precision, Recall, and F1 Score [Internet]. Towards Data Science [cited 2023 Aug 10]. Available from: https://towardsdatascience.com/performance-metrics-confusion-matrix-precision-recall-and-f1-score-a8fe076a2262

[41] Heydarian, M., Doyle, T.E., Samavi, R., 2022. MLCM: Multi-label confusion matrix. IEEE Access. 10, 19083-19095.
DOI: https://doi.org/10.1109/ACCESS.2022.3151048

[42] Coefficient Kappa de Cohen (K) [Internet] [cited 2023 Aug 10]. Available from: https://www.irdp.ch/institut/coefficient-kappa-cohen-2039.html

[43] Abbas, A.W., Minallh, N., Ahmad, N., et al., 2016. K-Means and ISODATA clustering algorithms for landcover classification using remote sensing. Sindh University Research Journal-SURJ (Science Series). 48(2), 315-318.

[44] Mfondoum, A.H.N., Etouna, J., Nongsi, B.K., et al., 2016. Assessment of land degradation status and its impact in arid and semi-arid areas by correlating spectral and principal component analysis neo-bands. International Journal. 5(2),

1539-1560.

[45] NDBI—ArcGIS Pro [Internet] [cited 2023 May 19]. Available from: https://pro.arcgis.com/en/pro-app/latest/arcpy/spatial-analyst/ndbi.htm

[46] Shafaey, M.A., Salem, M.A.M., Ebied, H.M., et al. (editors), 2018. Deep learning for satellite image classification. International Conference on Advanced Intelligent Systems and Informatics; 2018 Sep 1-3; Cairo, Egypt. Cham: Springer International Publishing. p. 383-391.
DOI: https://doi.org/10.1007/978-3-319-99010-1_35

[47] Warf, B., 2014. Supervised classification. Encyclopedia of Geography. Sage: Thousand Oaks, California.
DOI: https://doi.org/10.4135/9781412939591.n1101

[48] Würsch, L., Hurni, K., Heinimann, A., 2017. Google Earth Engine Image Pre-processing Tool: User Guide [Internet] [cited 2022 Dec 13]. Available from: https://www.cde.unibe.ch/e65013/e542846/e707304/e707386/e707390/CDE_Pre-processingTool-UserGuide_eng.pdf

[49] El Imanni, H.S., El Harti, A., Bachaoui, E.M., et al., 2023. Multispectral UAV data for detection of weeds in a citrus farm using machine learning and Google Earth Engine: Case study of Morocco. Remote Sensing Applications: Society and Environment. 30, 100941.
DOI: https://doi.org/10.1016/J.RSASE.2023.100941

[50] Chen, H., Yunus, A.P., Nukapothula, S., et al., 2022. Modelling Arctic coastal plain lake depths using machine learning and Google Earth Engine. Physics and Chemistry of the Earth, Parts A/B/C. 126, 103138.
DOI: https://doi.org/10.1016/J.PCE.2022.103138

[51] Amani, M., Ghorbanian, A., Ahmadi, S.A., et al., 2020. Google earth engine cloud computing platform for remote sensing big data applications: A comprehensive review. IEEE Journal of Selected Topics in Applied Earth Observations and Remote Sensing. 13, 5326-5350.
DOI: https://doi.org/10.1109/JSTARS.2020.3021052

[52] Tassi, A., Vizzari, M., 2020. Object-oriented lulc classification in google earth engine combining snic, glcm, and machine learning algorithms. Remote Sensing. 12(22), 3776.
DOI: https://doi.org/10.3390/rs12223776

Appendix

Table A1. Land cover evaluation metrics of each classifier.

SVM				
	PA	UA	OA	Kappa
Water_area	100	100		
Barren_area	100	77.35		
Forest_area	82.75	75	83	0.78
Built-up_area	69.23	81.81		
Cropped_area	50	86.66		
Cart				
	PA	UA	OA	Kappa
Water_area	100	100		
Barren_area	95.12	97.5		
Forest_area	89.65	81.25	91.50	0.89
Built-up_area	76.92	83.33		
Cropped_area	92.30	92.30		

Table A1 continued

RF				
	PA	UA	OA	Kappa
Water_area	100	100		
Barren_area	97.56	100		
Forest_area	93.10	90	95.42	0.94
Built-up_area	84.61	91.66		
Cropped_area	100	92.85		
GTB				
	PA	UA	OA	Kappa
Water_area	100	100		
Barren_area	97.56	100		
Forest_area	79.31	92	93.46	0.91
Built-up_area	88.46	79.31		
Cropped_area	100	92.85		
DT				
	PA	UA	OA	Kappa
Water_area	100	100		
Barren_area	95.12	97.5		
Forest_area	89.65	81.25	91.50	0.89
Built-up_area	76.92	83.33		
Cropped_area	92.30	92.30		
MD				
	PA	UA	OA	Kappa
Water_area	100	100		
Barren_area	95.12	100		
Forest_area	86.20	92.59	94.77	0.93
Built-up_area	92.30	88.88		
Cropped_area	100	89.65		